



# COMMUNICATIONS CHEMISTRY

## ARTICLE

<https://doi.org/10.1038/s42004-019-0214-4>

OPEN

## Asphaltene oxide promotes a broad range of synthetic transformations

Hyosic Jung <sup>1,2</sup> & Christopher W. Bielawski <sup>1,2,3</sup>

Carbocatalysts, which are catalytically-active materials derived from carbon-rich sources, are attractive alternatives to metal-based analogs. Graphene oxide is a prototypical example and has been successfully employed in a broad range of synthetic transformations. However, its use is accompanied by a number of practical and fundamental drawbacks. For example, graphene oxide undergoes explosive decomposition when subjected to elevated temperatures or microwaves. We found that asphaltene oxide, an oxidized collection of polycyclic aromatic hydrocarbons that are often discarded from petroleum refining processes, effectively overcomes the drawbacks of using graphene oxide in synthetic chemistry and constitutes a new class of carbocatalysts. Here we show that asphaltene oxide may be used to promote a broad range of transformations, including Claisen-Schmidt condensations, C-C cross-couplings, and Fischer indole syntheses, as well as chemical reactions which benefit from the use of microwave reactors.

<sup>1</sup>Center for Multidimensional Carbon Materials (CMCM), Institute for Basic Science (IBS), Ulsan 44919, Republic of Korea. <sup>2</sup>Department of Chemistry, Ulsan National Institute of Science and Technology (UNIST), Ulsan 44919, Republic of Korea. <sup>3</sup>Department of Energy Engineering, Ulsan National Institute of Science and Technology (UNIST), Ulsan 44919, Republic of Korea. Correspondence and requests for materials should be addressed to C.W.B. (email: [bielawski@unist.ac.kr](mailto:bielawski@unist.ac.kr))

The burgeoning field of carbocatalysis<sup>1</sup>, defined as transformations that are promoted by materials composed primarily of carbon, offers a number of attractive features, particularly when compared to metal-based analogs. For example, carbocatalysts often are comparatively inexpensive, require less laborious workup procedures due to their heterogeneous nature, and exhibit relatively low degrees of toxicity without sacrificing activity and/or reactivity. While charcoal<sup>2</sup>, carbon nanotubes (CNTs)<sup>3</sup>, and buckminsterfullerene (C<sub>60</sub>)<sup>4</sup> (see Fig. 1), have historically found utility in select reactions, the field experienced rapid growth after it was discovered that the high chemical potential of graphene oxide (GO) may be harnessed to drive synthetic transformations. Indeed, GO has been shown to facilitate oxidations<sup>5</sup>, reductions<sup>6</sup>, C–C cross couplings<sup>7,8</sup>, and many other useful chemical reactions<sup>9</sup>. The broad reactivity displayed by GO is due, in part, to the myriad of different oxygen-containing functional groups that populate its surface coupled with a relatively high acidity (pH 3.0 at 1.0 mg mL<sup>-1</sup> in water)<sup>10</sup>.

Despite these advantages, GO and other carbocatalysts suffer from a number of fundamental and practical drawbacks. Because GO is a berthollide and features (i) myriad oxygen-containing functional groups, (ii) a range of surface areas that depend in part on the extent of exfoliation, and/or (iii) indeterminate edge and basal structures, the origin(s) of the catalytic activities remain largely unknown. GO has also been found to undergo rapid decomposition when exposed to elevated temperatures, light, or microwaves, presumably due to its relatively high oxygen content (the C/O ratio of GO is typically ~2)<sup>11</sup>.

We posited that solutions to the drawbacks described above may be realized through the discovery of new carbon precursors derived from asphaltene, a residual material comprised of the

heavier, aromatic components of crude oil<sup>12</sup>. Due to potential benefits that include enhanced production efficiency, lower transportation costs, and higher fuel quality, efforts toward the study of asphaltene have focused primarily on methods that facilitate extraction and removal during oil refining processes<sup>13</sup>. Because it is a mixture of various aromatic structures, asphaltene is typically classified in terms of its solubility in toluene and not by its chemical structure<sup>14</sup>. However, recent results using atomic force microscopy (AFM), have clarified the components of asphaltene<sup>15</sup> to be mixtures of polycyclic aromatic hydrocarbons (PAHs). Since the truncated structures that were observed are comparable to 2D carbons, asphaltene was termed ‘nanographene’ and thus was envisioned to serve as a small molecular model of graphite/graphene.

Previous reports of oxidizing asphaltene to facilitate its separation from crude oil<sup>14</sup> or to reduce bitumen viscosity<sup>16</sup> have shown that treatment with potassium permanganate<sup>14</sup> or ozone<sup>16</sup> resulted in increased hydrophilicity, which ultimately facilitated precipitation from oil. We hypothesized that such oxidized derivatives of asphaltene, termed asphaltene oxide (AO), may function as economically viable catalysts due to the low cost of the precursor while providing insights into the intrinsic chemistry displayed by GO and other carbocatalysts<sup>17</sup>. Moreover, we reasoned that the relatively small size of AO may not only facilitate the elucidation of the catalytically active sites on other oxidized carbons but also accelerate expansion of the field of carbocatalysis.

Herein, we report the synthesis of AO and describe the utility of this material in various transformations. We also provide new insight to the origins of the activities displayed by GO, an area of intense interest, and demonstrate how AO may be used in applications that are inaccessible to other carbocatalysts.

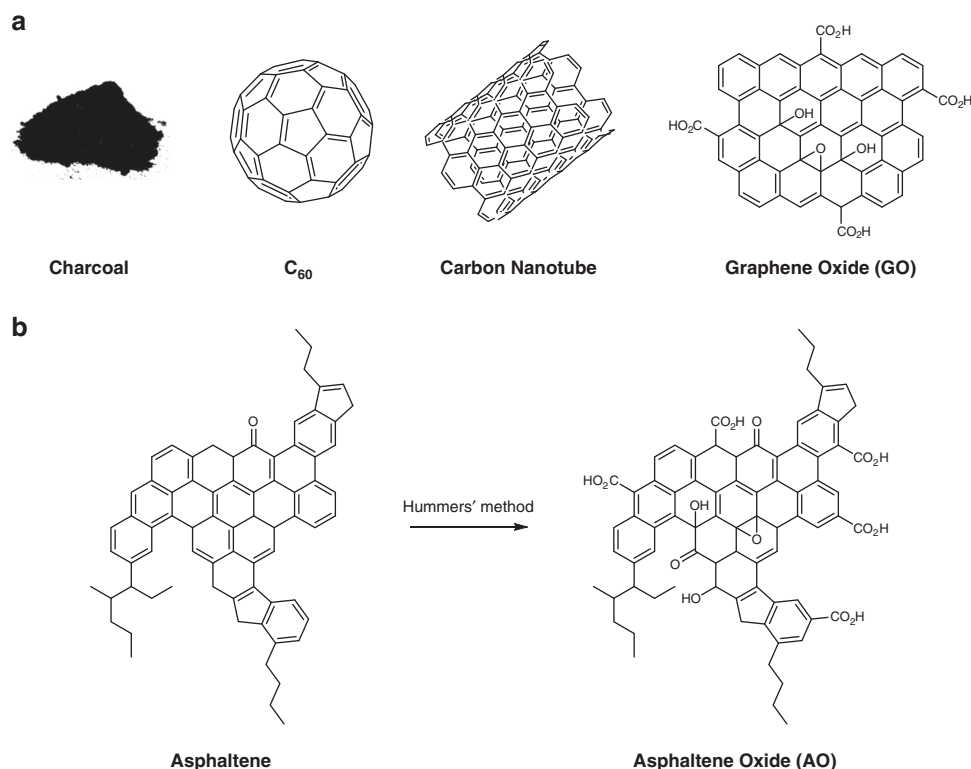


**Fig. 1** Examples of catalytically active carbon materials. **a** Representative pictures or structures of typical carbocatalysts, including charcoal, buckminsterfullerene (C<sub>60</sub>), a carbon nanotube (CNT) and graphene oxide (GO). **b** Oxidation of asphaltene using Hummers' method affords asphaltene oxide (AO)

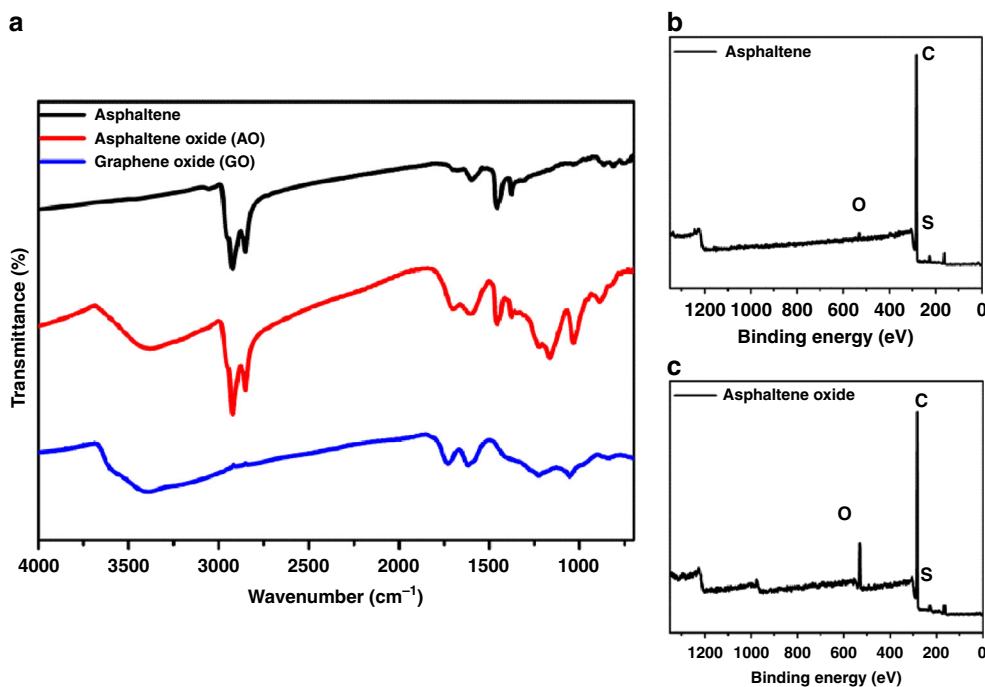


**Fig. 2** Summary of characterization data. **a** FT-IR spectra recorded for asphaltene (black line), AO (red line), and GO (blue line). **b** XPS survey spectrum recorded for asphaltene. **c** XPS survey spectrum recorded for AO

## Results

**Synthesis of asphaltene oxide.** Our initial efforts were directed toward synthesizing AO using Hummers' method<sup>18</sup>, which is commonly used to oxidize graphite to GO. Asphaltene was treated with a 1:4.3 w/w mixture of sulfuric acid and potassium permanganate at 35 °C for 3 h, and then washed with an aqueous solution of HCl (1.0 M) followed by deionized water to extract heavy metal impurities (e.g., vanadium and nickel)<sup>19</sup>. The resulting product featured a relatively high oxygen content (~13.1 wt%; c.f., a ~1.4 wt% oxygen content that was measured for the starting material), as determined using elemental analysis (see Supplementary Table 1), as well as strong IR absorption bands that were assigned to hydroxyl ( $\nu_{\text{O-H}} = 3400 \text{ cm}^{-1}$ ), carbonyl ( $\nu_{\text{C=O}} = 1700 \text{ cm}^{-1}$ ), and epoxide ( $\nu_{\text{C-O}} = 1220$  and  $1160 \text{ cm}^{-1}$ ) stretching frequencies (see Fig. 2a). X-ray photoelectron spectroscopy (XPS) survey spectra also showed that the oxygen content of AO was significantly higher than that of the asphaltene starting material and signals consistent with the aforementioned structural assignments were observed (see Fig. 2b, c).

To quantify the functional groups present on AO, a series of chemical tests were devised. As summarized in Fig. 3, the reagents utilized were designed to preferentially react with either the resident carboxylic acid, hydroxy or epoxide groups, and contained nitrile handles to facilitate characterization via IR spectroscopy and elemental analysis (Supplementary Figs. 1–2). For example, treatment of AO with 3-cyanobenzyl alcohol under Steglich esterification conditions<sup>20</sup> afforded the corresponding ester derivative as determined in part by the observation of a bathochromic shift of the carbonyl stretching frequency ( $\nu_{\text{C=O}}$ , from  $1700 \text{ cm}^{-1}$  to  $1650 \text{ cm}^{-1}$ ) and the appearance of a new signal that was assigned to a nitrile group ( $\nu_{\text{C}\equiv\text{N}} = 2225 \text{ cm}^{-1}$ ). The corresponding carbamate derivative was obtained by condensing AO with 3-cyanophenyl isocyanate. The intensity of the hydroxyl stretching frequency ( $\nu_{\text{O-H}} = 3400 \text{ cm}^{-1}$ ) measured in the AO starting material decreased as new, strong signals that were assigned to nitrile ( $\nu_{\text{C}\equiv\text{N}} = 2225 \text{ cm}^{-1}$ ), amido ( $\nu_{\text{N-H}} =$

$3070 \text{ cm}^{-1}$ ) and carbamyl ( $\nu_{\text{C=O}} = 1550 \text{ cm}^{-1}$ ) groups formed. Finally, treatment of AO with malononitrile under basic conditions resulted in the ring-opening of the epoxide groups<sup>21</sup>, as evidenced in part by an increased intensity of a signal assigned to the hydroxyl groups ( $\nu_{\text{O-H}} = 3400 \text{ cm}^{-1}$ ) and the disappearance of signals attributed to the epoxide groups ( $\nu_{\text{C-O}} = 1230 \text{ cm}^{-1}$ ) in the AO starting material. The new product also exhibited a new  $\nu_{\text{C}\equiv\text{N}}$  at  $2180 \text{ cm}^{-1}$ . Using elemental analysis data recorded for the modified AOs, the constituent functional groups were quantified and compared to those identified in GO, which were also determined by analyzing the compositions of derivatives that were obtained from an analogous set of chemical tests (see Table 1). The differences in accessible functional groups measured for AO and GO was attributed to the relative small size of the former and effectively explain why differential reactivities were observed (vide infra). Further support for this hypothesis was obtained by determining that the pH of a suspension of AO in water ( $[\text{AO}]_0 = 1.0 \text{ mg mL}^{-1}$ ) was 3.5; for comparison, a pH of 3.0 was recorded when GO was subjected to otherwise identical conditions<sup>22</sup>.

**Etherifications using AO.** The conversion of alcohols to their corresponding aldehydes/ketones (oxidation) or ethers (condensation) often serve as benchmark transformations for carbocatalysts<sup>5</sup>. As such, our initial efforts were directed toward exploring the chemistry of AO with benzyl alcohol. A series of reactions were performed under neat conditions that included varying the catalyst loading (5–20 wt%) as well as the temperature (100–150 °C). As summarized in Table 2, AO preferentially facilitated condensations in lieu of oxidations. Indeed, benzyl alcohol was successfully converted to benzyl ether in yields of up to 82% using a 10 wt% loading of AO at 150 °C for 3 h. Likewise, subjecting AO to a range of alcohols that featured different functional groups afforded the expected ethers (see Supplementary Table 5). While electron-rich substrates generally resulted in higher conversions than their electron-deficient analogs, an observation consistent with an acid-catalyzed process, the unique

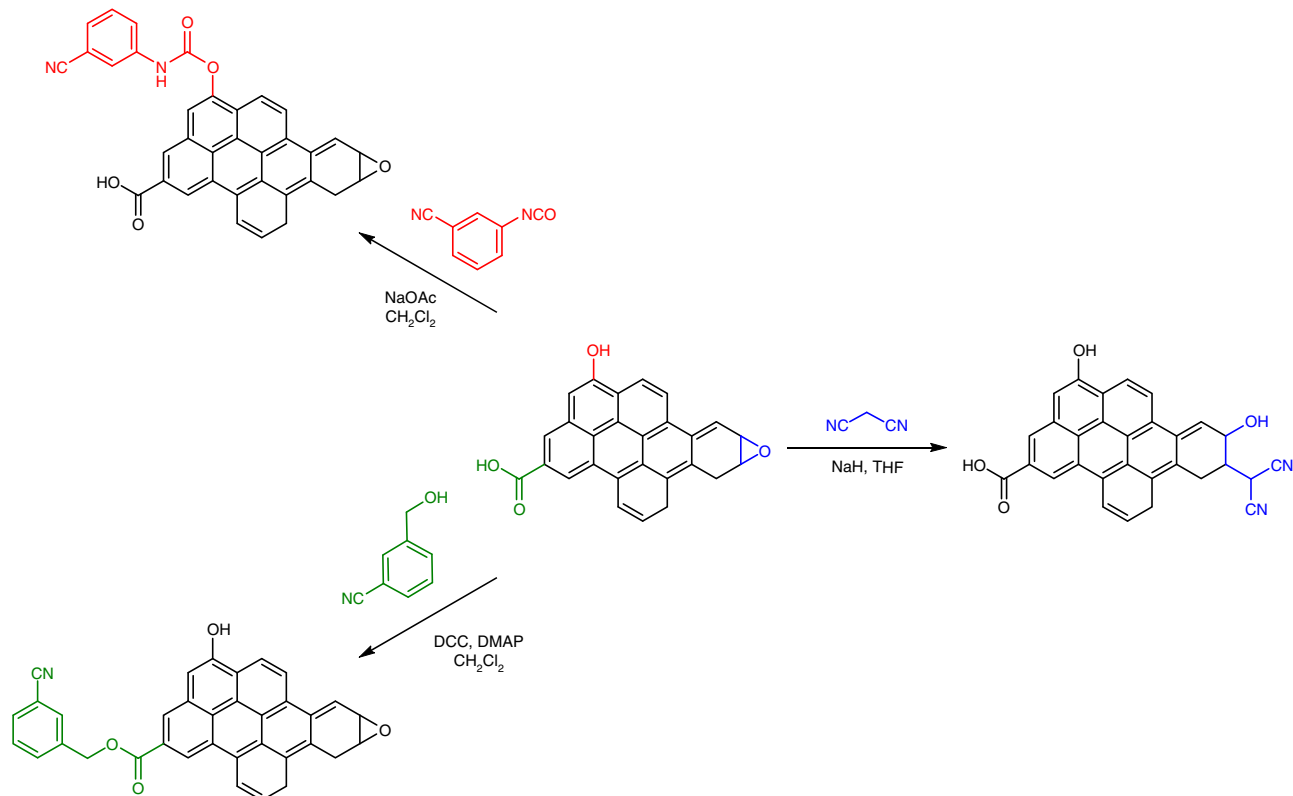


**Fig. 3** Chemical tests used to quantify the functional groups displayed on GO and AO. The starting material shown in the center represents a truncated form of GO or AO and features pendant carboxylic acid, hydroxy, and epoxide groups. Using the reagents shown, the carboxylic acid groups were converted to esters, the hydroxyl groups were converted to carbamates, and the epoxide groups were ring-opened. In all cases, the corresponding products feature cyano groups (CN) that could be quantified using IR spectroscopy as well as elemental analyses.

**Table 1** Summary of functional group quantification data obtained for AO and GO<sup>a</sup>

Functional group	AO (mol/g)	GO (mol/g)
Carboxylic acid	$>2.3 \times 10^{-3}$	$>3.6 \times 10^{-4}$
Hydroxy	$>1.4 \times 10^{-3}$	$>1.1 \times 10^{-4}$
Epoxide	$>5.4 \times 10^{-4}$	$>1.2 \times 10^{-3}$

<sup>a</sup>The calculations were based on the elemental analysis data (see Supplementary Table 2 and Supplementary Table 3)

structure and composition exhibited by AO prominently affected the reaction. In accord with results reported for GO<sup>23</sup> heating mixtures of benzyl alcohol or electron-rich derivatives thereof to 200 °C in the presence of AO afforded the corresponding poly(phenylene methylene)s in good yields (see Supplementary Table 8) and established the carbon-material as a useful polymerization catalyst.

As part of an effort to identify the nature of the catalytically active acid sites in AO, a series of control reactions were performed. To test the hypothesis that the aforementioned condensation chemistry was promoted by an acid, benzyl alcohol was treated with AO in the presence of excess base (i.e., pyridine)<sup>24,25</sup>. Product formation was not observed under these conditions, presumably due to neutralization, and thus reinforced the notion that the catalytically active sites were acidic. Since the elemental analysis data revealed that AO contained sulfur, it was reasoned that sulfonic acids may be present on the surface and

contribute to the catalytic activity observed. To test this supposition, benzenesulfonic acid (pH 2.3 at 1.0 mg mL<sup>-1</sup> in water), which was envisioned to represent sulfonic acid groups on AO, was introduced to benzyl alcohol under optimized reaction conditions. Benzyl ether was not observed as a product and, instead, a polymeric material was obtained. An analogous etherification reaction performed with mellitic acid, a discrete organic acid (pH 2.4 at 1.0 mg mL<sup>-1</sup> in water) with a relatively large C/O ratio (1:1), also did not afford benzyl ether as a product. Although vanadium (ca. 50 ppm) and nickel (ca. 30–200 ppm) were detected in AO using inductively coupled plasma optical emission spectrometry (ICP-OES) and atomic absorption spectrometry (AAS), control experiments that were performed with asphaltene, which was also found to contain vanadium and nickel in similar concentrations as AO, indicated that the trace metals did not significantly influence the catalytic activity.

To determine the fate of AO after the aforementioned transformations and to assess its recyclability, the catalyst was collected after an etherification reaction with benzyl alcohol and then re-used. Due to its low solubility in organic solvents, AO was conveniently recovered by filtration in yields of up to 95%. Although the recovered AO exhibited a lower C/O ratio than that measured for the starting material (14:1 vs. 7:1, respectively; see Supplementary Table 7), IR signals assigned to hydroxyl and carbonyl stretching frequencies were retained (see Supplementary Fig. 3). The recovered material was successfully and repeatedly used over multiple cycles to facilitate condensations with minimal loss in activity (see Supplementary Table 6). For example, benzyl ether was obtained in a 70% yield from benzyl alcohol using a catalyst that was subjected to five (5) successive reactions

**Table 2** Condensation of benzyl alcohol under various conditions<sup>a</sup>

Catalyst	Catalyst loading (wt%)	Temperature (°C)	Benzyl ether <sup>b</sup> (%)	Benzaldehyde <sup>b</sup> (%)
AO	5	100	10	0
AO	5	120	41	0
AO	5	150	61	6
AO	10	100	17	0
AO	10	120	60	0
AO	10	150	82	9
AO	20	100	24	0
AO	20	120	68	0
AO	20	150	73	7
--	--	150	0	<10
Asphaltene	20	150	0	0
Mellitic acid	20	150	0	0
AO + Pyridine <sup>c</sup>	10	150	0	0
PhSO <sub>3</sub> H	10	150	0	0

<sup>a</sup>Unless otherwise noted, all reactions were performed with benzyl alcohol using the indicated catalyst loading and temperature for 3 h (see Supplementary Table 4 for reaction time optimization)

<sup>b</sup>Conversion of benzyl alcohol to benzyl ether or benzaldehyde was calculated by <sup>1</sup>H NMR spectroscopy against a standard (18-crown-6)

<sup>c</sup>10 wt% AO and 0.1 mL of pyridine

(conditions per cycle: 10 wt% cat. loading, 150 °C, and 3 h); for comparison, a yield of 80% was obtained after the first cycle.

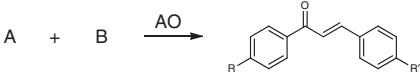
**Claisen–Schmidt condensations.** Building on these results, we next explored the use of AO in other acid-catalyzed condensations<sup>26</sup>. Efforts were directed toward Claisen–Schmidt-type reactions to obtain chalcones, which are valuable products that commonly form the basis of many pharmaceutical agents<sup>27</sup>. As summarized in Table 3, condensation of various benzaldehydes and acetophenones, including electron-rich and electron-deficient derivatives, afforded the expected products in good yields (up to 78%; see Table 3, entries 1–5). Considering that the mechanism of the Claisen–Schmidt-type reaction entails dehydration, we explored the ability of AO to catalyze multiple transformations in tandem. After discovering that phenylacetylene underwent hydration in high yields (86%) when treated with AO at 100 °C for 24 h (see Supplementary Table 9), efforts were directed toward the coupling of terminal alkynes with aldehydes. We reasoned that the water formed upon condensation may hydrate the alkynes in situ and the resulting ketones may then undergo further reactions. To confirm our hypothesis, equimolar quantities of phenylacetylene and an electron-rich or deficient benzaldehyde were heated in the presence of AO. The aforementioned substrates underwent tandem-hydration-aldol condensation and the expected chalcone products were obtained in reasonable isolated yields over the two steps (up to 48%; see Table 3, entries 6–8).

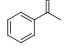
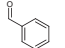
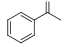
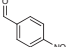
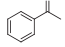
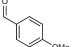
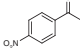
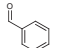
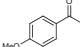
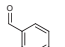
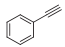
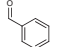
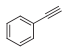
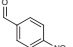
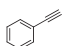
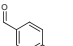
**Metal-free C–C cross couplings.** Next, our efforts with AO were directed toward catalyzing C–C cross coupling reactions which have historically been accomplished with the aid of metal catalysts, such as those based on palladium and/or copper<sup>28</sup>. Acidic carbon-based materials, including GO<sup>7,8</sup>, have also been shown to be effective in facilitating C–C bond forming reactions with certain substrates. For example, xanthene is prone to oxidation in air and the resulting species can be converted to a xanthenyl cation via a GO-catalyzed dehydration, enabling nucleophilic attack<sup>29</sup>. As summarized in Table 4, AO was found to be an effective catalyst for coupling veratrole to xanthene. In general,

the results obtained using AO were found to be competitive to those reported for GO under similar conditions and catalyst loadings. Moreover, good yields of the coupled product were obtained in the presence or absence of co-catalysts (e.g., tosylic acid monohydrate; TsOH·H<sub>2</sub>O) that are commonly used in such transformations.

**Exploring the origins of catalyst activity.** The effects of elemental composition, catalyst loading, and particle size on catalytic activity<sup>30</sup> were deconvoluted and compared to the results obtained from analogous experiments using GO<sup>18</sup>. We selected the cross-coupling chemistry described above as the basis for the analysis because AO and GO operated in a similar manner. The particle sizes of GO and AO employed in these experiments were measured to be 1400 nm and 40 nm, respectively, using dynamic light scattering (DLS). Since using identical quantities (20 mg) of AO or GO afforded similar yields of the same cross-coupled product, (9-(3,4-dimethoxyphenyl)-9H-xanthene), (63% vs. 66%, respectively; lit.<sup>7</sup> 67%), we concluded that particle size and catalyst loading were not key determinants of reaction performance. However, a positive correlation between elemental composition and catalytic activity was observed. Although the C/O ratios of GO and AO were measured to be 1.5 and 6.7, respectively, the latter afforded a higher yield of product (27% vs. 63%) when the loadings of the catalyst were normalized to their respective oxygen contents (see Supplementary Table 10). Similar outcomes were obtained when the reactions were performed without added co-catalyst (16% vs. 40%). Thus, we concluded that the activities displayed by these catalysts were not defined exclusively by their absolute oxygen content and attribute the enhanced activity displayed by AO to its relatively high C/O ratio.

**Microwave enhanced chemistry.** While GO has garnered extraordinary interest as a carbocatalyst, its utility can be restricted. For example, it is widely known that GO undergoes rapid and extensive reduction upon exposure to elevated temperatures and/or microwave irradiation<sup>31,32</sup> and, in some cases, it has been reported to explode under such conditions<sup>33</sup> due to the formation of gaseous byproducts, including CO<sub>2</sub>, CO, and H<sub>2</sub>O. Indeed,

**Table 3 A summary of various AO-catalyzed condensations used to prepare chalcones**


Entry	A	B	Yield <sup>(c)</sup> (%)
1 <sup>[a]</sup>			72
2 <sup>[a]</sup>			78
3 <sup>[a]</sup>			70
4 <sup>[a]</sup>			63
5 <sup>[a]</sup>			44
6 <sup>[a]</sup>			43
7 <sup>[a]</sup>			40
8 <sup>[a]</sup>			48

<sup>a</sup>All products were purified using column chromatography. NMR spectra are available in Supplementary Figs. 5–9  
<sup>b</sup>Aldol condensations were performed neat in 1:1 stoichiometry (0.5 mmol each) of ketone and aldehyde using 50.0 mg of AO at 80 °C for 16 h  
<sup>c</sup>Hydration-aldol condensations were performed neat in 1:1 stoichiometry (0.5 mmol each) of alkyne and aldehyde using 50.0 mg of AO at 100 °C for 16 h

despite the prevalence of microwave enhanced chemistry<sup>34</sup>, safety concerns may have stymied the exploration of the utility carbocatalysts in such capacities. Since AO can be considered as a truncated analog of GO with a lower oxygen content and a smaller size, we reasoned that such a material may be more amenable and safer for utilization in microwave-assisted reactions.

When a mixture of benzyl alcohol and AO were exposed to microwave irradiation, an increase in conversion of benzyl alcohol to benzyl ether as well as a decrease in reaction time was observed when compared to an analogous thermal reaction. For example, benzyl ether was obtained in a 90% yield from benzyl alcohol within 15 min when the condensation was conducted in a microwave reactor (see Supplementary Table 11); for comparison, 3 h was required when the same reaction mixture was heated in a oil bath (150 °C). Microwave irradiation also enabled expansion of the scope of suitable substrates (see Supplementary Table 12). For example, 4-methoxy benzyl alcohol was successfully converted to its respective ether in good yield (80%) under microwave conditions whereas product formation was not observed at elevated temperatures. Similar to GO, which is known to undergo reduction upon microwave irradiation<sup>35</sup>, a decrease in the oxygen weight percentage of AO was observed after it was used in a microwave reaction (c.f., 13.1% in the starting material to 9.3% in the recovered catalyst).

Regardless, the recovered AO retained its activity and was successfully used to facilitate microwave-promoted etherification over multiple cycles (see Supplementary Table 13). For comparison, subjecting benzyl alcohol to GO under similar conditions afforded benzyl ether and benzaldehyde in 53% and 6% yield, respectively. The oxygen content of the GO underwent significant reduction (from 42.5 to 9.3 wt%) and a large material expansion was observed (see Supplementary Fig. 4).

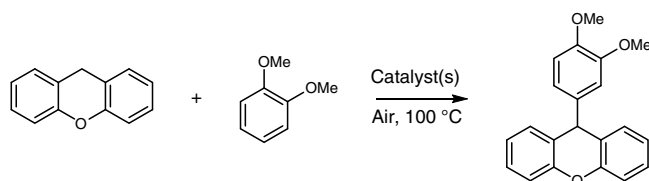
To further explore the potential of microwave-assisted carbocatalysis, the Fischer indole synthesis, a reaction commonly employed to prepare biologically active heterocycles, was selected<sup>36</sup>. As shown in Fig. 4, condensation of phenylhydrazine with cyclohexanone afforded the corresponding annulated indole in 44% isolated yield after 1 h at 100 °C under microwave irradiation. For comparison, 18 h were required to obtain the same yield of product in a conventional reactor at the same temperature. An improved yield of 62% was achieved when the reaction was conducted at 150 °C in a microwave reactor.

## Discussion

It was demonstrated that an oxidized form of asphaltene, an inexpensive petroleum byproduct, may be used to promote chemical transformations. Indeed, AO was found to be an effective carbocatalyst for a wide range of condensations, polymerizations, cross-couplings, cyclizations and other useful synthetic reactions. Asphaltene oxide functions primarily as an acid catalyst, whereas other carbocatalysts, including GO, often facilitates a range of reactions that can be non-discerning and thus affords mixtures of products through competing mechanisms (i.e., oxidation vs. dehydration). Moreover, due to its relatively small size and unique composition, AO was successfully used in a microwave reactor, the first example of its kind for a carbocatalyst, and a series of reactions were found to be significantly promoted under such conditions. The results described herein (i) establish asphaltene oxide and potentially other truncated forms of oxidized carbons as effective catalysts for facilitating chemical reactions and (ii) demonstrate that the unique structure and composition of AO enable applications that have hitherto not been possible with other oxidized carbons reported in the literature.

## Methods

**General considerations.** All reagents were purchased from Sigma Aldrich, Alfa-Aesar, TCI or Acros Organics, and used as received. Asphaltene (blown asphalt 5–10) was kindly supplied by Korea Petroleum. Unless otherwise noted, all experiments were performed under ambient conditions. NMR spectra were recorded on a Bruker Ascend 400 MHz spectrometer. Chemical shifts are reported in parts per million ( $\delta$ ). All NMR spectra were recorded in CDCl<sub>3</sub> and the residual solvent was referenced to 7.26 ppm. The following abbreviations apply: s, singlet; d, doublet; t, triplet; q, quartet; m, multiplet; br, broad. FT-IR spectra were recorded using KBr pellets on a Perkin-Elmer Frontier MIR spectrometer. Elemental analyses were performed using a Thermo Scientific Flash 2000 Organic Elemental Analyzer that was calibrated with 2,5-bis(5-*tert*-butyl-benzoxazol-2-yl)thiophene (BBOT). XPS data were recorded over a spot size of 500  $\mu$ m using an Escalab 250Xi (Thermo Fisher Scientific, Waltham, MA, USA) equipped with a monochromated aluminum K $\alpha$  source (1486.6 eV). All measurements were recorded at an angle normal to the surface using charge compensation via a combined ion/flood gun operating at a current of 50  $\mu$ A and an ion voltage of 2 V. Survey spectra were taken at a pass energy of 100 eV (10 scans). Calibration of the spectra was conducted by initially recording the gold 4f<sub>7/2</sub> spectrum of a gold foil. The peak position of the gold 4f<sub>7/2</sub> spectrum was then shifted to 84.0 eV and the shifted value was applied to all subsequent spectra. Polystyrene equivalent molecular weights and polydispersity index (*D*) values were measured by gel permeation chromatography (GPC) using a Malvern GPCmax Solvent/Sample Module. All samples were analyzed using THF as the eluent at a flow rate of 0.8 mL min<sup>-1</sup>. Mass spectrometry (MS) data were recorded on a Thermo LCQ Fleet Quadrupole Ion Trap Mass Spectrometer in Atmospheric Pressure Chemical Ionization (APCI) mode (electrospray voltage 3.5 kV). Atomic absorption spectroscopy (AAS) measurements were recorded on an Analytik Jena contraAA 800 D. Inductively coupled plasma optical emission spectroscopy (ICP-OES) measurements were recorded on a Varian 700-ES. All

**Table 4 Summary of C-C cross coupling reactions<sup>a</sup>**

Entry	TsOH·H <sub>2</sub> O (×10 <sup>-2</sup> mmol)	Catalyst	Reaction time (h)	Yield <sup>b</sup> (%)
1	1.0	AO	24	63
2	1.0	GO	24	66
3	1.0	AO	30	76
4 <sup>c</sup>	-	AO	24	40
5 <sup>c</sup>	-	GO	24	45
6 <sup>c</sup>	-	Asphaltene	24	0

<sup>a</sup>Unless otherwise noted, all reactions were performed with xanthene (0.5 mmol), veratrole (1.0 mmol), 20.0 mg of catalyst and TsOH·H<sub>2</sub>O (1.0 × 10<sup>-2</sup> mmol) as a co-catalyst at 100 °C for 24 h

<sup>b</sup>Isolated yields after purification using column chromatography

<sup>c</sup>Reaction was performed without a co-catalyst. Representative NMR data can be found in Supplementary Fig. 10

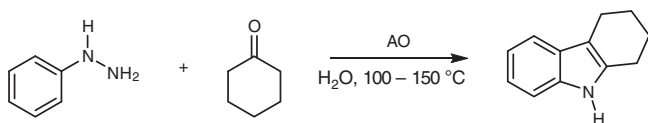


**Fig. 4** A Fischer indole synthesis using AO. Relatively high yields were obtained when the reaction was performed in a microwave reactor. See Supplementary Fig. 11 for the corresponding NMR data

microwave reactions were conducted using an Anton Paar GmbH-Monowave 300 microwave reactor.

**Separation of asphaltene.** Asphaltene (10.0 g) was mixed with *n*-heptane (2.0 L) and then sonicated. The mixture was filtered through a 0.22 μm nylon membrane and washed with *n*-heptane (0.5 L × 3). The filtered asphaltene particles were collected, dried under vacuum at 80 °C for 1 day, and then used without additional purification.

**Preparation of asphaltene oxide.** A 500 mL jacked reaction flask was cooled to 0 °C and then charged with asphaltene (4.0 g), concentrated sulfuric acid (0.1 L), and a stir bar. KMnO<sub>4</sub> (8.0 g) was subsequently slowly added to the flask over 2 h with stirring. The mixture was stirred at 0 °C for 15 min and then at 35 °C for an additional 3 h. The flask was cooled to 10 °C and deionized water (0.8 L) was added slowly to the mixture (CAUTION: this step was found to be exothermic!). The mixture was transferred to a beaker and then a 35% aqueous solution of H<sub>2</sub>O<sub>2</sub> (12.0 mL) was added to the aqueous mixture. The resulting black particles were filtered through a 0.22 μm nylon membrane and washed with 1 M HCl (0.8 L). The particles were then washed with deionized water until the pH of the filtered solution became 6–7. The filtered solids were collected and dried under vacuum at 50 °C for 1 day. The final product (3.8 g) was obtained as a black powder.

**Identification and quantification of carboxylic acids on AO and GO.** A 100 mL Schlenk flask was charged with 50.0 mg of AO or GO, 10.0 mL of CH<sub>2</sub>Cl<sub>2</sub> and a stir bar under an atmosphere of N<sub>2</sub>. The suspension was sonicated in a bath sonicator. After 30 min, 3-cyanobenzyl alcohol (200.0 mg, 1.5 mmol) and 4-(dimethylamino)pyridine (DMAP, 10.0 mg, 0.1 mmol) were added to the flask and the resulting mixture was cooled to 0 °C in an ice bath. In a separate flask, N,N'-dicyclohexylcarbodiimide (DCC; 155.0 mg, 0.8 mmol) was dissolved in 5.0 mL of CH<sub>2</sub>Cl<sub>2</sub>. The DCC solution was added dropwise to flask containing AO at 0 °C. The combined mixture was stirred at 25 °C for 24 h and then filtered. The isolated solids were washed with CH<sub>2</sub>Cl<sub>2</sub>, water and acetone, and then dried under vacuum for 1 day. The final product (51.7 mg), which was termed 'modified AO-1' (mAO-1) or 'modified GO-1' (mGO-1), respectively, was obtained as a black powder and characterized using FT-IR spectroscopy as well as elemental analysis. A new nitrile stretching frequency at 2225 cm<sup>-1</sup> was observed in the FT-IR spectrum recorded

for the product and the carbonyl signal initially measured in the AO starting material (1700 cm<sup>-1</sup>) shifted to 1650 cm<sup>-1</sup>.

**Identification and quantification of hydroxyl groups on AO and GO.** A 100 mL round bottom flask was charged with 50.0 mg of AO or GO, 10.0 mL of CH<sub>2</sub>Cl<sub>2</sub> and a stir bar. The suspension was sonicated for 30 min in a bath sonicator. Sodium acetate (123.0 mg, 1.5 mmol) and 3-cyanophenyl isocyanate (216.2 mg, 1.5 mmol) were subsequently added, and the resulting mixture was then stirred at 25 °C for 24 h. After filtration, the collected solids were washed with CH<sub>2</sub>Cl<sub>2</sub>, water and acetone, and then dried under vacuum for 1 day. The final product (52.3 mg), which was termed 'modified AO-2' (mAO-2) or 'modified GO-2' (mGO-2), respectively, was obtained as a black powder and characterized using FT-IR spectroscopy as well as elemental analysis. The FT-IR spectrum recorded for the product revealed an attenuated hydroxyl stretching frequency (3400 cm<sup>-1</sup>) as well as strong absorptions that were attributed to the nitrile (2225 cm<sup>-1</sup>), amido (3070 cm<sup>-1</sup>), and carbamyl (1550 cm<sup>-1</sup>) groups expected from the condensation product.

**Identification and quantification of epoxide groups on AO and GO.** A 50 mL flask was charged with sodium hydride (82.0 mg, 3.4 mmol), malononitrile (220.0 mg, 3.3 mmol) and 30.0 mL of THF under N<sub>2</sub> atmosphere. The mixture was stirred for 10 min. A separate 100 mL Schlenk flask was charged with 40.0 mg of AO or GO, 10.0 mL of THF and a stir bar under an atmosphere of N<sub>2</sub>. The suspension was sonicated for 30 min in a bath sonicator. After cooling both mixtures on an ice bath, the malononitrile solution was added dropwise to the AO suspension at 0 °C. The resulting mixture was then heated at 60 °C for 24 h and then filtered. The collected solids were washed with water, methanol and acetone, and then dried under vacuum for 1 day. The final product (43.7 mg), which was termed 'modified AO-3' (mAO-3), or 'modified GO-3' (mGO-3), respectively, was obtained as a black powder and characterized using FT-IR spectroscopy as well as elemental analysis. The FT-IR spectrum recorded for the product revealed the presence of a signal that was assigned to a nitrile group (2180 cm<sup>-1</sup>). In addition, when compared to the spectrum recorded for the AO starting material, the intensity of the signal assigned to the hydroxyl stretching frequency (3400 cm<sup>-1</sup>) increased while the signal assigned to the epoxide groups (1230 cm<sup>-1</sup>) disappeared upon inspection of the spectrum recorded for the product.

**General etherification procedure.** A Teflon-capped 8 mL vial was charged with 100.0 mg of benzyl alcohol, 5–20 wt% of AO, 18-crown-6 as a standard, and a stir bar. The vial was sealed under ambient atmosphere with Teflon tape. The vial was then heated to a pre-determined temperature (100–150 °C) for 3–12 h. To monitor the extent of the etherification reaction, aliquots were periodically removed and analyzed by NMR spectroscopy. Conversion was determined by integrating protons assigned to the standard (δ 3.69 ppm; s, 24 H) vs. the benzylic protons of benzyl alcohol (δ 4.70 ppm; s, 2 H) and benzyl ether (δ 4.57 ppm; s, 4 H). The products were not isolated.

**General dehydrative polymerization procedure.** A Teflon-capped 8 mL vial was charged with 500.0 mg of a benzyl alcohol, 50.0 mg of AO (10 wt%), and a stir bar. The vial was sealed under ambient atmosphere with Teflon tape. The vial was

heated at 200 °C for 24 h. The resulting mixture was cooled to room temperature and then filtered to remove the catalyst using CH<sub>2</sub>Cl<sub>2</sub>. The filtrate was concentrated and poured into excess methanol. The precipitate was collected and dried under vacuum (66% yield). Spectroscopic data were in accord with literature reports<sup>23</sup>.

**General aldol condensation procedure.** A Teflon-lined 8 mL vial was charged with 0.5 mmol of acetophenone, 0.5 mmol of aldehyde, 50.0 mg of AO, and a stir bar. The vial was sealed under ambient atmosphere with Teflon tape. The vial was heated at 80 °C for 16 h. The resulting mixture was cooled to room temperature and then filtered to remove the catalyst using CH<sub>2</sub>Cl<sub>2</sub> as the filtrate. Subsequent collection of the filtrate followed by evaporation of the residual solvent afforded the crude product, which was further purified using column chromatography (ethyl acetate: *n*-hexane, 1:9 v/v as eluent). Spectroscopic data were in accord with literature values<sup>37</sup>.

**General hydration-aldol condensation procedure.** A Teflon-capped 8 mL vial was charged with phenylacetylene (51.1 mg, 0.5 mmol), 0.5 mmol of aldehyde, 50.0 mg of AO and a stir bar. The vial was sealed under ambient atmosphere with Teflon tape. The vial was heated at 100 °C for 16 h. The resulting mixture was cooled to room temperature, and then filtered to remove the catalyst with the aid of CH<sub>2</sub>Cl<sub>2</sub>. The filtrate was collected, the residual solvent was evaporated, and the crude product was purified using column chromatography (ethyl acetate: *n*-hexane, 1:9 v/v as eluent). Spectroscopic data were in accord with literature values<sup>37</sup>.

**General C-C cross coupling procedure.** A Teflon-capped 8 mL vial was charged with xanthene (91.1 mg, 0.5 mmol), veratrole (138.2 mg, 1.0 mmol), TsOH·H<sub>2</sub>O (19.0 mg, 1.0 × 10<sup>-2</sup> mmol), AO (20.0 mg) and a stir bar. The vial was heated to 100 °C for 24 h while being left open to air. The resulting mixture was cooled to room temperature and then filtered to remove the catalyst using CH<sub>2</sub>Cl<sub>2</sub>. The filtrate was collected, the CH<sub>2</sub>Cl<sub>2</sub> was evaporated, and the crude mixture was purified using column chromatography (ethyl acetate: *n*-hexane, 1:9 v/v as eluent) to afford the desired product in 63% yield. Spectroscopic and analytical data were in accord with literature values<sup>26</sup>. <sup>1</sup>H NMR (400 MHz, CDCl<sub>3</sub>): δ 7.23–7.19 (t, 2 H), δ 7.13–7.11 (d, 2 H), δ 7.06–7.00 (d, 2 H), δ 6.98–6.96 (t, 2 H), δ 6.79–6.78 (d, 2 H), δ 6.65 (s, 1 H), δ 5.19 (s, 1 H), δ 3.84 (s, 3 H), δ 3.75 (s, 3 H). LR-MS (APCI): Calcd. For C<sub>21</sub>H<sub>18</sub>O<sub>3</sub> [M – H]<sup>+</sup>: 317.12; Found: 317.33.

**Microwave-promoted etherification procedure.** A Teflon-capped 10 mL microwave vial was charged with 100.0 mg of benzyl alcohol, 10 wt% of AO, and a stir bar. The vial was then microwaved at 150 °C for 5–30 min. To monitor the extent of the reaction, aliquots were periodically removed and analyzed by NMR spectroscopy against an external standard (18-crown-6). Conversions were determined by integrating protons attributed to the external standard (δ 3.69 ppm; s, 24 H) vs. the benzylic protons of benzyl alcohol (δ 4.70 ppm; s, 2 H) and benzyl ether (δ 4.57 ppm; s, 4 H).

**Microwave-promoted Fischer indole synthesis procedure.** A Teflon-capped 10 mL microwave vial was charged with phenylhydrazine (129.8 mg, 1.2 mmol), cyclohexanone (98.2 mg, 1.0 mmol), AO (100.0 mg), water (2.0 mL) and a stir bar. The vial was then microwaved at 150 °C for 1 h. The resulting mixture was cooled to room temperature and then filtered to remove the catalyst. After the filtrate was extracted with water and CH<sub>2</sub>Cl<sub>2</sub>, the organic phase was dried over MgSO<sub>4</sub> and then purified using column chromatography (ethyl acetate: *n*-hexane, 1:9 v/v as eluent) to afford the desired product in 62% yield. Spectroscopic and analytical data were in accord with literature values<sup>38</sup>. <sup>1</sup>H NMR (400 MHz, CDCl<sub>3</sub>): δ 7.64 (s, 1 H), δ 7.46–7.44 (d, 1 H), δ 7.29–7.27 (d, 1 H), δ 7.14–7.07 (m, 2 H), δ 2.74–2.70 (m, 4 H), δ 1.91–1.87 (m, 4 H).

## Data availability

The authors declare that the main data supporting the findings of this study are available within the article and its Supplementary Information.

Received: 10 June 2019 Accepted: 22 August 2019

Published online: 25 September 2019

## References

- Dreyer, D. R. & Bielawski, C. W. Carbocatalysis: heterogeneous carbons finding utility in synthetic chemistry. *Chem. Sci.* **2**, 1233–1240 (2011).
- Alkhazov, T. G., Lisovskii, A. E. & Gulakhmedova, T. K. Oxidative dehydrogenation of ethylbenzene over a charcoal catalyst. *React. Kinet. Catal. Lett.* **12**, 189–193 (1979).
- Zhang, J. et al. Surface-modified carbon nanotubes catalyze oxidative dehydrogenation of *n*-butane. *Science* **322**, 73–77 (2008).
- Li, B. & Xu, Z. A nonmetal catalyst for molecular hydrogen activation with comparable catalytic hydrogenation capability to noble metal catalyst. *J. Am. Chem. Soc.* **131**, 16380–16382 (2009).
- Dreyer, D. R., Jia, H. P. & Bielawski, C. W. Graphene oxide: a convenient carbocatalyst for facilitating oxidation and hydration reactions. *Angew. Chem. Int. Ed.* **49**, 6813–6816 (2010).
- Primo, A., Neatu, F., Florea, M., Parvulescu, V. & Garcia, H. Graphenes in the absence of metals as carbocatalysts for selective acetylene hydrogenation and alkene hydrogenation. *Nat. Commun.* **5**, 5291 (2014).
- Wu, H. et al. Graphene-oxide-catalyzed direct CH-CH-type cross-coupling: the intrinsic catalytic activities of zigzag edges. *Angew. Chem. Int. Ed.* **57**, 10848–10853 (2018).
- Morioku, K., Morimoto, N., Takeuchi, Y. & Nishina, Y. Concurrent formation of carbon-carbon bonds and functionalized graphene by oxidative carbon-hydrogen coupling reaction. *Sci. Rep.* **6**, 25824 (2016).
- Hu, F. et al. Graphene-catalyzed direct friedel-crafts alkylation reactions: Mechanism, selectivity, and synthetic utility. *J. Am. Chem. Soc.* **137**, 14473–14480 (2015).
- Dreyer, D. R., Todd, A. D. & Bielawski, C. W. Harnessing the chemistry of graphene oxide. *Chem. Soc. Rev.* **43**, 5288–5301 (2014).
- Kudin, K. N. et al. Raman spectra of graphite oxide and functionalized graphene sheets. *Nano. Lett.* **8**, 36–41 (2008).
- Groenzin, H. & Mullins, O. C. Asphaltene molecular size and structure. *J. Phys. Chem. A* **103**, 11237–11245 (1999).
- Groenzin, H. & Mullins, O. C. Molecular size and structure of asphaltenes from various sources. *Energy Fuels* **14**, 677–684 (2000).
- Choi, S., Byun, D. H., Lee, K., Kim, J. D. & Nho, N. S. Asphaltene precipitation with partially oxidized asphaltene from water/heavy crude oil emulsion. *J. Petrol. Sci. Eng.* **146**, 21–29 (2016).
- Schuler, B., Meyer, G., Pena, D., Mullins, O. C. & Gross, L. Unraveling the molecular structures of asphaltenes by atomic force microscopy. *J. Am. Chem. Soc.* **137**, 9870–9876 (2015).
- Choi, S., Choi, S. Q., Kim, J. D. & Nho, N. S. Partially oxidized asphaltene as a bitumen viscosity reducer. *Energy Fuels* **31**, 9240–9246 (2017).
- Su, C. & Loh, K. P. Carbocatalysts: graphene oxide and its derivatives. *Acc. Chem. Res.* **46**, 2275–2285 (2013).
- Hummers, W. S. & Offeman, R. E. Preparation of graphitic oxide. *J. Am. Chem. Soc.* **80**, 1339–1339 (1958).
- Yakubov, M. R. et al. Concentrations of vanadium and nickel and their ratio in heavy oil asphaltenes. *Pet. Chem.* **56**, 16–20 (2016).
- Neises, B. & Steglich, W. Simple method for the esterification of carboxylic acids. *Angew. Chem. Int. Ed.* **17**, 522–524 (1978).
- Collins, W. R., Schmois, E. & Swager, T. M. Graphene oxide as an electrophile for carbon nucleophiles. *Chem. Commun.* **47**, 8790–8792 (2011).
- Dimiev, A. M., Alemany, L. B. & Tour, J. M. Graphene oxide: origin of acidity, its instability in water, and a new dynamic structural model. *ACS Nano* **7**, 576–588 (2013).
- Dreyer, D. R., Jarvis, K. A., Ferreira, P. J. & Bielawski, C. W. Graphite oxide as a dehydrative polymerization catalyst: A one-step synthesis of carbon-reinforced poly(phenylene methylene) composites. *Macromolecules* **44**, 7659–7667 (2011).
- Dhakshinamoorthy, A., Alvaro, M., Concepcion, P., Fornes, V. & Garcia, H. Graphene oxide as an acid catalyst for the room temperature ring opening of epoxides. *Chem. Commun.* **48**, 5443–5445 (2012).
- Dhakshinamoorthy, A., Alvaro, M., Puche, M., Fornes, V. & Garcia, H. Graphene oxide as catalyst for the acetalization of aldehydes at room temperature. *ChemCatChem* **4**, 2026–2030 (2012).
- Jia, H. P., Dreyer, D. R. & Bielawski, C. W. Graphite Oxide as an auto-tandem oxidation-hydration-aldol coupling catalyst. *Adv. Synth. Catal.* **353**, 528–532 (2011).
- Aponte, J. C. et al. Synthesis, cytotoxicity, and anti-trypanosoma cruzi activity of new chalcones. *J. Med. Chem.* **51**, 6230–6234 (2008).
- Shen, G. et al. Palladium-copper catalyzed C(sp<sup>3</sup>)-C(sp<sup>2</sup>) bond C-H activation cross-coupling reaction: Selective arylation to synthesize 9-aryl-9H-xanthene and 9,9-diaryl-xanthene derivatives. *RSC Adv.* **6**, 84748–84751 (2016).
- Schweitzer-Chaput, B. et al. Synergistic effect of ketone and hydroperoxide in Bronsted acid catalyzed oxidative coupling reactions. *Angew. Chem. Int. Ed.* **52**, 13228–13232 (2013).
- Navalon, S., Dhakshinamoorthy, A., Alvaro, M., Antonietti, M. & Garcia, H. Active sites on graphene-based materials as metal-free catalysts. *Chem. Soc. Rev.* **46**, 4501–4529 (2017).
- Chen, W. F., Yan, L. F. & Bangal, P. R. Preparation of graphene by the rapid and mild thermal reduction of graphene oxide induced by microwaves. *Carbon* **48**, 1146–1152 (2010).
- Chiu, P. L. et al. Microwave- and nitronium ion-enabled rapid and direct production of highly conductive low-oxygen graphene. *J. Am. Chem. Soc.* **134**, 5850–5856 (2012).



33. Shulga, Y. M. et al. Carbon nanomaterial produced by microwave exfoliation of graphite oxide: new insights. *RSC Adv.* **4**, 587–592 (2014).
34. Dallinger, D. & Kappe, C. O. Microwave-assisted synthesis in water as solvent. *Chem. Rev.* **107**, 2563–2591 (2007).
35. Zhu, Y. W. et al. Microwave assisted exfoliation and reduction of graphite oxide for ultracapacitors. *Carbon* **48**, 2118–2122 (2010).
36. Mohammadi Ziarani, G., Moradi, R., Ahmadi, T. & Lashgari, N. Recent advances in the application of indoles in multicomponent reactions. *RSC Adv.* **8**, 12069–12103 (2018).
37. Dai, W. et al. Highly efficient oxidation of alcohols catalyzed by a porphyrin-inspired manganese complex. *Chem. Commun.* **51**, 11268–11271 (2015).
38. Xu, D. Q. et al. Fischer indole synthesis catalyzed by novel SO<sub>3</sub>H-functionalized ionic liquids in water. *Green. Chem.* **11**, 1239–1246 (2009).

### Acknowledgements

The Institute for Basic Science (IBS-R019) and the BK21 Plus Program as funded by the Ministry of Education and the National Research Foundation of Korea are acknowledged for support. We are grateful to Ms. Hyunkyong Jo for assistance with graphic design.

### Author contributions

H.J. performed the experiments and data analyses. C.W.B. designed and supervised the project. Both authors contributed to the development of the paper.

### Additional information

Supplementary information accompanies this paper at <https://doi.org/10.1038/s42004-019-0214-4>.

**Competing interests:** The authors declare no competing interests.

**Reprints and permission** information is available online at <http://npg.nature.com/reprintsandpermissions/>

**Publisher's note** Springer Nature remains neutral with regard to jurisdictional claims in published maps and institutional affiliations.



**Open Access** This article is licensed under a Creative Commons Attribution 4.0 International License, which permits use, sharing, adaptation, distribution and reproduction in any medium or format, as long as you give appropriate credit to the original author(s) and the source, provide a link to the Creative Commons license, and indicate if changes were made. The images or other third party material in this article are included in the article's Creative Commons license, unless indicated otherwise in a credit line to the material. If material is not included in the article's Creative Commons license and your intended use is not permitted by statutory regulation or exceeds the permitted use, you will need to obtain permission directly from the copyright holder. To view a copy of this license, visit <http://creativecommons.org/licenses/by/4.0/>.

© The Author(s) 2019